Flexible Piezoelectric Touch Sensor by Alignment of Lead-Free Alkaline Niobate Microcubes in PDMS

Deutz, Daniella B.; Mascarenhas, Neola T.; Schelen, J. Ben J.; de Leeuw, Dago M.; van der Zwaag, Sybrand; Groen, Pim

DOI
10.1002/adfm.201700728

Publication date
2017

Document Version
Accepted author manuscript

Published in
Advanced Functional Materials

This is an Accepted Manuscript of an article published by Wiley in Advanced Functional Materials on 24-04-2017,
available online: http://dx.doi.org/10.1002/adfm.201700728

Flexible piezoelectric touch sensor by alignment of lead-free alkaline niobate microcubes in PDMS

Daniella B. Deutz, Neola T. Mascarenhas, Ben Schelen, Dago M. de Leeuw, Sybrand van der Zwaag and Pim Groen*

D. B. Deutz, N. T. Mascarenhas, J. B. J. Schelen, Prof. dr. D. M. de Leeuw, Prof. dr. S. van der Zwaag, Prof. dr. W. A. Groen
Delft University of Technology, Kluyverweg 1, 2629HS Delft, the Netherlands
E-mail: daniella.deutz@gmail.com

Keywords: piezoelectric, touch sensors, energy harvesting, functional composites, alkaline niobates

Abstract A highly sensitive, lead-free and flexible piezoelectric touch sensor is reported based on composite films of alkaline niobate $K_{0.485}Na_{0.485}Li_{0.03}NbO_3$ (KNLN) powders aligned in a polydimethylsiloxane (PDMS) matrix. KNLN powder was fabricated by solid-state sintering and consists of microcubes. The particles were dispersed in uncured PDMS and oriented by application of a dielectrophoretic alignment field. The dielectric constant of the composite film is almost independent of the microstructure, while upon alignment the piezoelectric charge coefficient increases more than ten fold up to 17 pC N^{-1}. A quantitative analysis shows that the origin is a reduction of the inter-particle distance to under 1.0 μm in the aligned bi-continuous KNLN chains. The temperature stable piezoelectric voltage coefficient exhibits a maximum value of 220 mV m N^{-1}, at a volume fraction of only 10%. This state-of-the-art value outperforms bulk piezoelectric ceramics and composites with randomly dispersed particles, and is comparable to the values reported for the piezoelectric polymers PVDF and P(VDF-TrFE). Optimized composite films are incorporated in flexible piezoelectric touch sensors. The high sensitivity is analyzed and discussed. As the fabrication technology is straightforward and easy to implement, applications are foreseen in flexible electronics such wireless sensor networks and biodiagnostics.

1. Introduction

Piezoelectric materials have the remarkable ability to convert tensile and compressive stresses into electric charge, and vice versa. Applications that make use of the direct effect, where mechanical stress yields an electric voltage, or of the converse piezoelectric effect, where an electric voltage is generated upon mechanical deformation, are widespread and range from actuators, through sensors, to energy harvesters.[1-4] Here we use piezoelectric materials to realize a sensitive, flexible touch sensor, where a voltage is generated upon a dynamical change in applied force.

When a piezoelectric capacitor is poled perpendicular to the electrodes, and stressed and charge tapped in the same direction, a short circuit current, I_{SC}, is generated:

$$I_{SC} = \frac{Q}{\Delta t} = \frac{d_{33}\Delta F}{\Delta t} \tag{1}$$

where Q is the generated charge, $\Delta F/\Delta t$ is the change in applied force over time, and d_{33} is the piezoelectric charge coefficient, given in pC N^{-1}. The open circuit voltage, V_{OC}, is then derived as:

$$V_{OC} = \frac{Q}{C} = \frac{d_{33}\Delta F}{\varepsilon_r \varepsilon_0 A / l} = \left(\frac{d_{33}}{\varepsilon_r \varepsilon_0}\right) l \frac{\Delta F}{A} = g_{33} l \Delta P \tag{2}$$

where C is the capacitance, A the area and l the thickness of the capacitor. ε_0 is the permittivity of free space and ε_r is the relative dielectric constant of the piezoelectric material. Equation 2 shows that the open circuit voltage linearly depends on the change in applied pressure, ΔP, and the thickness of the piezoelectric material. The proportionality constant is the figure of merit of the sensor, *viz.* the piezoelectric voltage coefficient, g_{33}, defined as $d_{33}/\varepsilon_0\varepsilon_r$ and expressed in mV m N^{-1}.

Most piezoelectric materials consist of inorganic ceramics. They exhibit large piezoelectric charge coefficients, over 500 pC N^{-1}, but the high value of the dielectric constant severely limits their piezoelectric voltage coefficient.[5,6] Furthermore, ceramics are inherently brittle and, therefore, cannot be applied in a flexible touch sensor. To that end a piezoelectric polymer is required.[7,8,9] We note that high values of the voltage coefficient have been

reported for ferroelectret polymers, *i.e.* soft electroactive films,[10-12] but applications are hampered by discharging at elevated temperature.[13] The most widely studied,[14,15] commercially available,[16] polymer is the piezoelectric homopolymer polyvinylidenefluoride (PVDF) and its random copolymer with trifluoroethylene (P(VDF-TrFE)). The state-of-the-art piezoelectric voltage coefficient is about 200 mV m N^{-1}. The coercive field, however, is 60 MV m^{-1}.[15] Poling films with a thickness of more than 100 μm, needed to generate a measurable voltage output, *c.f.* Equation 2, then requires high poling voltages of more than 6 kV. Another drawback is the low Curie temperature, which for the commonly used copolymer P(VDF-TrFE) (65/35) is only 100 °C.

Hence, there is a need in flexible electronics for a touch sensor that combines the mechanical flexibility of a polymer with a high piezoelectric voltage coefficient and a low coercive field. Here we show that a solution for this material selection problem can be provided by aligned ceramic-polymer composites. Random composites are hardly piezoelectric as an applied electric field is confined by the low dielectric constant of the polymer matrix.[17-21] However, upon aligning ceramic particles in a polymer matrix, the piezoelectric charge coefficient dramatically increases. As the dielectric constant of the composite film remains small, dominated by that of the matrix, the system can exhibit a large g_{33} value.

Dielectrophoresis has proven to be a well-suited technique to align a piezoelectric ceramic filler as the active phase, into a low dielectric polymer matrix as passive phase.[22-24] Aligned composite films have been reported with piezoelectric voltage coefficients attaining 120 mV m N^{-1}.[25,26] The Curie temperature remains, in first order approximation, that of the ceramic filler. The main drawback of these composites is that the voltage coefficient lags behind that of PVDF and of P(VDF-TrFE).

To improve the piezoelectric voltage coefficient, we use composites consisting of a piezoelectric ceramic filler inside a low stiffness matrix of polydimethylsiloxane (PDMS). As filler we use lead-free alkaline niobate microcubes, $K_{0.485}Na_{0.485}Li_{0.03}NbO_3$ (KNLN),[27-30] rendering the touch sensor biocompatible. A state-of-the-art high piezoelectric voltage coefficient of 220 mV m N^{-1} is realized by aligning the piezoelectric particles using dielectrophoresis. The implementation in a sensitive touch sensor is demonstrated and the system performance is analyzed and discussed.

2. Fabrication of KNLN-PDMS composite films

KNLN-PDMS composite films[31-35] were prepared by mixing the KNLN microcubes in an optically clear two-component polydimethylsiloxane (PDMS) polymer, (Sylgard 184, Dow Corning), at a volume of 0 to 20 %, in a planetary speed mixer (DAC 150 FVZ, Hauschild, Germany). The slurry was degassed, poured into a prepared Teflon mold and clamped between two steel plates.

The KNLN microcubes were aligned in the uncured PDMS by dielectrophoresis, as schematically depicted in **Figure 1a**. An AC electric field of 2 kV mm^{-1} was used. The alignment efficiency of dielectrophoresis can be inferred from the phase angle between applied voltage and leakage current at the dielectrophoresis frequency. The frequency was varied from 1 mHz to 10 kHz. The optimal frequency is obtained when the phase angle in the uncured composite slurry is 90 °. The system then is almost purely capacitive, with minimal leakage current. However, typical phase angles for these systems are as low as 50 – 60 ° depending on the electrical properties of matrix and filler, matrix viscosity, and filler morphology, showing incomplete alignment. Here at 200 Hz we have found an optimal phase angle of 88 ° which implies almost perfect alignment. We did not examine MHz range alignment, since the attained phase angle was already near perfectly out of phase.

As can be seen in **Video S1** in the Supporting Information, in the first 10 s, the KNLN microcubes reorient themselves parallel to the electric field lines. Subsequently, the cubes slowly link up into parallel chains. Effective alignment takes place in 60 s and no further particle movement can be distinguished.

After alignment, the composites were cured at 100 °C for 1 hour. The dielectrophoretic field remained turned on to prevent particle sedimentation. The particle alignment in the composite film can be inferred from the SEM micrograph of **Figure 1b**. The micron sized KNLN cubes are almost perfectly oriented in bi-continuous parallel chains, between the electrodes.

After curing, Au electrodes were applied on both sides of the films with a sputter coater (Quorum Q300T, East Sussex, UK). A photograph of the composite film is presented in **Figure 1c**. As prepared films are not piezoelectric as the ferroelectric polarization is not aligned. To render the films piezoelectric they were poled in a silicone oil bath at 150 °C, for 6 min at 7.5 kV mm^{-1}. We note that this field is an order of magnitude lower than the coercive

field of PVDF. Afterwards the films were cooled to ambient temperature in the presence of the poling field, and aged at room temperature for at least 24 hours before (piezo)electric measurement.

3. Piezoelectric constants of composite films

Figure 2a represents the measured piezoelectric charge coefficient, d_{33}, as a function of KNLN content. Open circles represent the values extracted for films with randomly dispersed particles, prepared without dielectrophoretic field. The films are hardly piezoelectric. However, the charge coefficient dramatically increases upon aligning the microcubes, as shown by the closed squares. The relative dielectric constant, ε_r, and the corresponding dielectric loss as a function of KNLN content are presented in **Figure 2c,d** respectively. The dielectric constant monotonically increases with KNLN content and is almost independent of the microstructure. Furthermore, the composite films remain highly resistive as can be inferred from the low value of the dielectric loss, which remains below 2 % for all compositions. From the measured values of the piezoelectric charge coefficient and the dielectric constant we calculated the piezoelectric voltage coefficient, g_{33}. The values are presented as a function of KNLN content in **Figure 2b**. The voltage coefficient peaks at a state-of-the-art value of 220 mV m N^{-1} at a KNLN content of only 10 vol.% in aligned composites. This value is more than one order of magnitude higher than that obtained for randomly dispersed particle composites[17-26,31-35] and on par with the values reported for the piezoelectric polymers PVDF and P(VDF-TrFE).[14-16]

The explanation for the increase in g_{33} is that d_{33} strongly depends on the intra-chain connectivity, while ε_r is a bulk property, proportional to the fill factor but almost independent of the microstructure. In random composites with low volume fractions of ceramic particles, the electric field is confined in the low dielectric constant polymer matrix. There is no electric field over the piezoelectric particles, which explains why d_{33} in random composites is very small.

There are many models to describe the dependence of ε_r and d_{33} on the volume fraction of two phase random ceramic-polymer composites.[36] Here we use the Yamada model, given by Equation 3 and 4 as:[21]

$$\varepsilon_{r_{Yamada}} = \varepsilon_p \left[1 + \frac{n\varphi\left(\varepsilon_{33_c} - \varepsilon_p\right)}{n\varepsilon_p + \left(1-\varphi\right)\left(\varepsilon_{33_c} - \varepsilon_p\right)} \right] \qquad (3)$$

$$d_{33_{Yamada}} = \frac{\alpha\varphi n\varepsilon_p}{n\varepsilon_p + \left(\varepsilon_{33_c} - \varepsilon_p\right)} d_{33_c} \tag{4}$$

where φ is the volume fraction of the ceramic particles and n is their aspect ratio, or shape factor. The sub-indices 'p' and 'c' stand for polymer and bulk ceramic respectively. The composite films are fully poled; hence the poling efficiency, α, is taken as unity. For the bulk values we use: a d_{33c} of 125 pC N^{-1}, ε_{33c} of 400 and ε_p of 3.9.[27-30]

The dotted lines in Figure 2a,c represent simultaneous fits of d_{33} and ε_r to the experimental data. A good agreement is obtained. Both d_{33} and ε_r increase with volume fraction. For the shape factor a value of 5.6 is extracted. This value implies a rectangular aspect ratio of the particles of 1.95, in fair agreement with the aspect ratio obtained from the SEM micrograph of the microcubes (*c.f.* Figure 1b).

In aligned composites the value of d_{33} remains small until at a high enough fill factor the first bi-continuous paths between the electrodes are formed. After this threshold, the value of d_{33} increases with the volume fraction of percolating paths. This behavior can quantitatively be described with the Bowen model for ε_r and the Van den Ende model for d_{33}, given by Equation 5 and 6 as:[22,24]

$$\varepsilon_{r_{DEP}} = \varphi\left[\frac{R\varepsilon_p\varepsilon_{33_c}}{\varepsilon_{33_c} + R\varepsilon_p}\right] + \left(1-\varphi\right)\varepsilon_p \tag{5}$$

$$d_{33_{DEP}} = \frac{\left(1+R\right)^2 \varepsilon_p \varphi Y_{33_c} d_{33_c}}{\left(\varepsilon_{33_c} + R\varepsilon_p\right)\left(\left(1+R\varphi\right)Y_{33_c} + \left(1-\varphi\right)RY_p\right)} \tag{6}$$

where R is the intra-chain connectivity, which is equal to the ratio of the mean particle size (*d50*) over the mean inter-particle distance within the bi-continuous chains. The fully drawn lines in Figure 2a,c represent simultaneous fits of d_{33} and ε_r to the experimental data. A good agreement is obtained for an intra-chain connectivity of 13. This value translates to a mean inter-particle distance in the aligned, percolating chains of less than 1 μm in fair agreement with the inter-particle distance observed in SEM micrographs (see Figure 1b). The dielectrophoretic alignment has a staggering effect on d_{33}. At 10 vol.% of filler, the value increases ten fold from 1.5 to 17 pC N^{-1}, which is due to the local increase in intra-chain connectivity leading to bi-continuous percolating paths.

In contrast to d_{33}, the dielectric constant, ε_r, experiences only a marginal increase due to alignment of the particles. The dielectric constant is dominated by that of the polymer matrix, does not depend on details of the microstructure, and increases linearly with the volume fraction of ceramic particles (see Figure 2c). Consequently, as shown in Figure 2b, the piezoelectric voltage coefficient, g_{33}, exhibits a maximum at very low volume fraction, around the percolation threshold.

4. Flexible touch sensor performance

For the aligned films with 10 vol.% KNLN that exhibit the optimal, state-of-the-art piezoelectric voltage coefficient, we examined the voltage output as a function of excitation form, pulsed or sinusoidal, applied force, frequency and temperature. We used a film with a thickness of 1.1 mm. The top two panels in **Figure 3a** show the force and the output voltage under sinusoidal excitation with peak to peak force of 1, 3 and 10 N. The bottom two panels show the force and voltage output under pulse excitation with 1, 3 and 10 N. Inserts show the form of a single sinusoidal excitation and pulse excitation and the corresponding changes in open circuit voltage at 1 N peak to peak. In both cases the output voltage increases linearly with applied force. Under sinusoidal excitation the open circuit voltage follows the change in applied pressure, according to Equation 2. Experimentally there is no overshoot, meaning that inelastic deformation can be disregarded. The extracted piezoelectric voltage coefficient, g_{33}, therefore perfectly agrees with the value of 220 mV m N^{-1} as presented in Figure 2b. In the pulse excitation an overshoot is detected, indicative of inelastic losses, and therefore the extracted value is slightly lower.

The voltage output is almost frequency independent. **Figure 3b** shows that the output voltage under a 5 N peak to peak sinusoidal force excitation, decreases from an average of 16.9 V peak to peak at 0.1 Hz to 16.0 V at 10 Hz. The frequency independence implies that the leakage current can be ignored, which is in perfect agreement with the low extracted value of the dielectric loss, as shown in Figure 2d. Compared to commercially available PVDF based polymer and PZT ceramic components the open circuit voltage output is significantly larger (**Figure S1)**. Furthermore, the voltage output is almost temperature independent. **Figure 3c** shows the open circuit voltage at temperatures from -10 to 50 °C; under a peak to peak excitation of 5 N the voltage remains at a steady level of about 16 V. This is expected as the voltage coefficient of KNLN is temperature independent far below the Curie temperature, which is about 420 °C,[27-30] and the measurements are performed far above the glass transition

temperature of PDMS of -120 °C and well below the onset of decomposition at 200 °C.

Furthermore the composite films are mechanically flexible. All the films exhibit elastomer-type behavior, with a Young's modulus of only 8.6 MPa, and a strain at break of 210 %. These values are similar to that of the elastomeric homopolymer PDMS, which is not surprising as the loading level is only 10 vol.%.

As the overall performance of the composite films is stable with time, frequency and temperature, and as the films are mechanically flexible, they could be integrated into a flexible, touch-sensitive patch, as shown in **Figure 4**. The flexible sensor patch contains three distinct 10 vol.% aligned KNLN-PDMS sensor buttons, which can be individually tapped. Each piezo button is terminated with a 10 MΩ load and this output voltage is amplified with 208x gain, as shown on the handheld oscilloscope. To suppress unwanted, out-of-band electrical noise the signal bandwidth is reduced by integration in the piezo's own capacitance and further limited with the bandwidth of the amplifier circuit. To improve the signal integrity, all connections are electronically shielded on both sides by Al tape stuck to a thin sheet of (pink) polyethylene. Figure 4 shows that upon touching the sensor, a clear output signal is produced on the oscilloscope. Even light tapping of the piezo button generates enough voltage to accurately distinguish variations in touch intensity and speed (see **Video S2**). We note that adding a dielectrophoretic processing step to arrive at a ceramic-polymer composite film is straightforward. Effectively a dense, flexible and large-area composite film can be produced in any shape that can be implemented into a flexible touch sensor.

5. Summary and conclusion

In summary, piezoelectric, flexible films were fabricated by dispersing lead-free piezoceramic $K_{0.485}Na_{0.485}Li_{0.03}NbO_3$ (KNLN) microcube powder into an elastomeric PDMS matrix. Before curing the films, the particles were aligned using an oscillating dielectrophoretic field. The dielectric constant of the composite films, ε_r, is almost independent of the microstructure, dominated by that of the PDMS matrix and increases linearly with filler fraction. On the other hand, upon aligning, the piezoelectric charge coefficient, d_{33}, increases more than ten fold, up to 17 pC N^{-1}. Quantitative analysis has shown that the origin is a reduction of the inter-particle distance to under 1.0 μm in the aligned bi-continuous chains. The piezoelectric voltage coefficient, g_{33}, exhibits a maximum value of 220 mV m N^{-1}, at a volume fraction of only 10 %. This value is more than one order of magnitude higher than that obtained for randomly

dispersed particle composites and comparable to values reported for the piezoelectric polymers PVDF and P(VDF-TrFE). These biocompatible, piezoelectric KNLN composite films combine the best of both worlds; the coercive field and the Curie temperature are dominated by that of the KNLN ceramics, while due to the low loading levels the mechanical properties resemble those of PDMS.

The composite films have been integrated into a flexible touch sensor. We have demonstrated the high sensitivity of the sensor under a controlled dynamical change of applied force via measuring the open circuit voltage, and by finger tapping a load matched and amplified flexible touch patch. Composite films, comprising aligned piezoelectric particles in a polymer matrix, are straightforward to fabricate. Hence, we anticipate that implementation of this approach will lead to new flexible sensor systems for temperature, infrared, impact and torque measurements. The developed sensor can replace brittle ceramic sensors and, therefore, can be applied in many fields where flexible electronics are needed, such as medical diagnostics and wireless sensors networks.

6. Experimental Section

$K_{0.485}Na_{0.485}Li_{0.03}NbO_3$ (KNLN) powders were prepared as described previously[25,26] from stoichiometric mixtures of the >99 % pure oxides $NaCO_3$, K_2CO_3, Li_2CO_3, and Nb_2O_5 (Sigma Aldrich), by milling with 5 mm yttria-stabilized ZrO_2 balls in cyclohexane. A two-step calcination scheme was employed by first calcining at 1050 °C for 3 hours, milling for 5 hours, and then calcining again at 950 °C for 20 hours. The powder was dried, sieved through a 63 μm size mesh and ultrasonicated to mitigate agglomeration. The final powder consists of microcubes with a medium diameter of the particle size distribution, *d50,* of 2.4 μm.

The piezoelectric charge coefficient, d_{33}, was measured with a Berlincourt type piezometer on poled capacitors (PM300, Piezotest, London, UK). A static force of 10 N was used, under a 0.25 N peak to peak sinusoidal excitation at 110 Hz. The capacitance, *C*, and dielectric loss were measured at 1 kHz and 1 V with an Agilent 4263B LCR meter (Santa Clara, CA, USA). ε_{33}, measured under zero stress, was derived from the capacitance. A tensile tester (Instron 3365, Darmstadt, Germany) was used to measure the Young's modulus and strain at break by uniaxial tensile testing at least 5 different samples at 23 °C.

The open circuit voltage, V_{OC}, was measured with a 6514 Keithley electrometer (Cleveland, OH, USA) by actuating disk-shaped sensors (8.7 mm diameter and 1.1 mm thickness) with a pin force supplied by an inductive voice coil. The dynamic pin force was controlled by an Agilent 33210A function generator (Santa Clara, CA, USA) driving the current amplifier for the inductive voice coil, and ranged from 1 to 10 N at 0.1 to 10 Hz. The sensors were clamped at a static force of 10 N between two rounded electrodes, identical to those used in the PM300 Berlincourt piezometer. The temperature was regulated by a MCPE1-07106NC-S Peltier element placed beneath the bottom electrode.

Supporting Information

Supporting Information is available from the Wiley Online Library or from the author.

Acknowledgements

We gratefully acknowledge financial support from the European Commission, FP7 NMP program, under grant no. 310311. We thank Jukka Riihiaho of the company aito-touch, Finland for collaboration on the flexible touch-sensitive patch, Ming Li of Delft University of Technology, for his assistance with thermogravimetric analysis of PDMS, and Vincent L. Stuber of Delft University of Technology for designing the Table of Contents figure.

References

[1] C. R. Bowen, H. A. Kim, P. M. Weaver, S. Dunn, *Energy Environ. Sci.* **2014**, *7*.

[2] J. F. Tressler, S. Alkoy, R. E. Newnham, *J. Electroceram.* **1998**, *2*, 4.

[3] K. Uchino, *Int. Cent. Actuators Transducers, Penn. State Univ.* **2003**, 40.

[4] H. A. Sodano, D. J. Inman, G. Park, *Shock Vib. Dig.* **2004**, *36*, 197.

[5] J. Rödel, K. G. Webber, R. Dittmer, W. Jo, M. Kimura, D. Damjanovic, *J. Eur. Ceram. Soc.* **2015**, *35*, 6.

[6] T. R. Shrout, S. J. Zhang, *J. Electroceramics* **2007**, *19*, 113.

[7] I. Graz, M. Krause, S. Bauer-Gogonea, S. Bauer, S. P. Lacour, B. Ploss, M. Zirkl, B. Stadlober, S. Wagner, *J. Appl. Phys.* **2009**, *106*.

[8] C. Rendl, P. Greindl, M. Haller, M. Zirkl, B. Stadlober, P. Hartmann, In *Proceedings of the 25th annual ACM symposium on User interface software and technology* **2012**, (pp. 509-518).

[9] T. Vuorinen, M. Zakrzewski, S. Rajala, D. Lupo, J. Vanhala, K. Palovuori, S. Tuukkanen, *Adv. Funct. Mater.* **2014**, *24*, 6340.

[10] S. Bauer, F. Bauer, In *Piezoelectricity: Evolution and Future of a Technology*; Springer Berlin Heidelberg: Berlin, Heidelberg, **2008**; pp. 157–177.

[11] S. Bauer, R. Gerhard-Multhaupt, G. M. Sessler, *Phys. Today* **2004**, *57*, 37.

[12] A. Mellinger, M. Wegener, W. Wirges, R. R. Mallepally, R. Gerhard-Multhaupt, *Ferroelectrics* **2006**, *331*, 189.

[13] W. Li, D. Torres, T. Wang, C. Wang, N. Sepulveda, *Nano Energy* **2016**, *30*, 649.

[14] T. Furukawa, *IEEE Trans. Electr. Insul.* **1989**, *24*, 375.

[15] I. Katsouras, K. Asadi, M. Li, T. B. van Driel, K. S. Kjær, D. Zhao, T. Lenz, Y. Gu, P. W. M. Blom, D. Damjanovic, M. M. Nielsen, D. M. de Leeuw, *Nat. Mater.* **2016**, *15*, 78.

[16] Piezotech S. A. S., Company Literaure, *Piezoelectric Films Technical Information*; **2012**, Hesingue, France.

[17] R. E. Newnham, D. P. Skinner, L. E. Cross, *Materials Research* **1978**, *13*.

[18] C. Dias, D. K. Das-Gupta, Y. Hinton, R. J. Shuford, *Sensors Actuators A Phys.* **1993**, *37–38*, 343.

[19] A. Peláiz-Barranco, P. Marin-Franch, *J. Appl. Phys.* **2005**, *97*, 34104.

[20] G. Sa-Gong, A. Safari, S. J. Jang, R. E. Newnham, *Ferroelectr. Lett. Sect.* **1986**, *5*, 131.

[21] T. Yamada, T. Ueda, T. Kitayama, *J. Appl. Phys.* **1982**, *53,* 6.

[22] C. P. Bowen, R. E. Newnham, C. A. Randall, *J. Mater. Res.* **1998**, *13*, 1.

[23] S. A. Wilson, G. M. Maistros, R. W. Whatmore, *J. Phys. D: Appl. Phys.* **2005**, *38*, 2.

[24] D. A. van den Ende, B. F. Bory, W. A. Groen, S. van der Zwaag, *J. Appl. Phys.* **2010**, *107*, 02410.

[25] N. K. James, D. B. Deutz, R. K. Bose, S. van der Zwaag, P. Groen, *J. Am. Ceram. Soc.* **2016**, *99*, 12.

[26] D. B. Deutz, N. T. Mascarenhas, S. van der Zwaag, W. A. Groen, *J. Am. Ceram. Soc.* **2016**, DOI: 10.1111/jace.14698.

[27] Y. Saito, H. Takao, T. Tani, T. Nonoyama, K. Takator, T. Homma, T. Nagaya, M. Nakamura, *Nature* **2004**,*432*.

[28] Y. Guo, K. Kakimoto, H. Ohsato, *Appl. Phys. Lett.* **2004**, *85*, 4121.

[29] S. Wongsaenmai, S. Ananta, R. Yimnirun, *Ceram. Int.* **2012**, *38*, 147.

[30] J.-F. Li, K. Wang, F.-Y. Zhu, L.-Q. Cheng, F.-Z. Yao, *J. Am. Ceram. Soc.* **2013**, *96*, 3677.

[31] C. K. Jeong, K.-I. Park, J. Ryu, G.-T. Hwang, K. J. Lee, *Adv. Funct. Mater.* **2014**, *24*, 2620.

[32] Q. Xue, Z. Wang, H. Tian, Y. Huan, Q.-Y. Xie, Y. Yang, D. Xie, C. Li, Y. Shu, X.-H. Wang, T.-L. Ren, *AIP Adv.* **2015**, *5*, 17102.

[33] M. K. Gupta, S.-W. Kim, B. Kumar, *ACS Appl. Mater. Interfaces* **2016**, *8*, 1766.

[34] Y. Yang, J. H. Jung, B. K. Yun, F. Zhang, K. C. Pradel, W. Guo, Z. L. Wang, *Adv. Mater.* **2012**, *24*, 5357.

[35] J. H. Jung, C.-Y. Chen, B. K. Yun, N. Lee, Y. Zhou, W. Jo, L.-J. Chou, Z. L. Wang, *Nanotechnology* **2012**, *23*, 375401.

[36] M. C. Araújo, C. M. Costa, S. Lanceros-Méndez, *J. Non. Cryst. Solids* **2014**, *387*, 6.

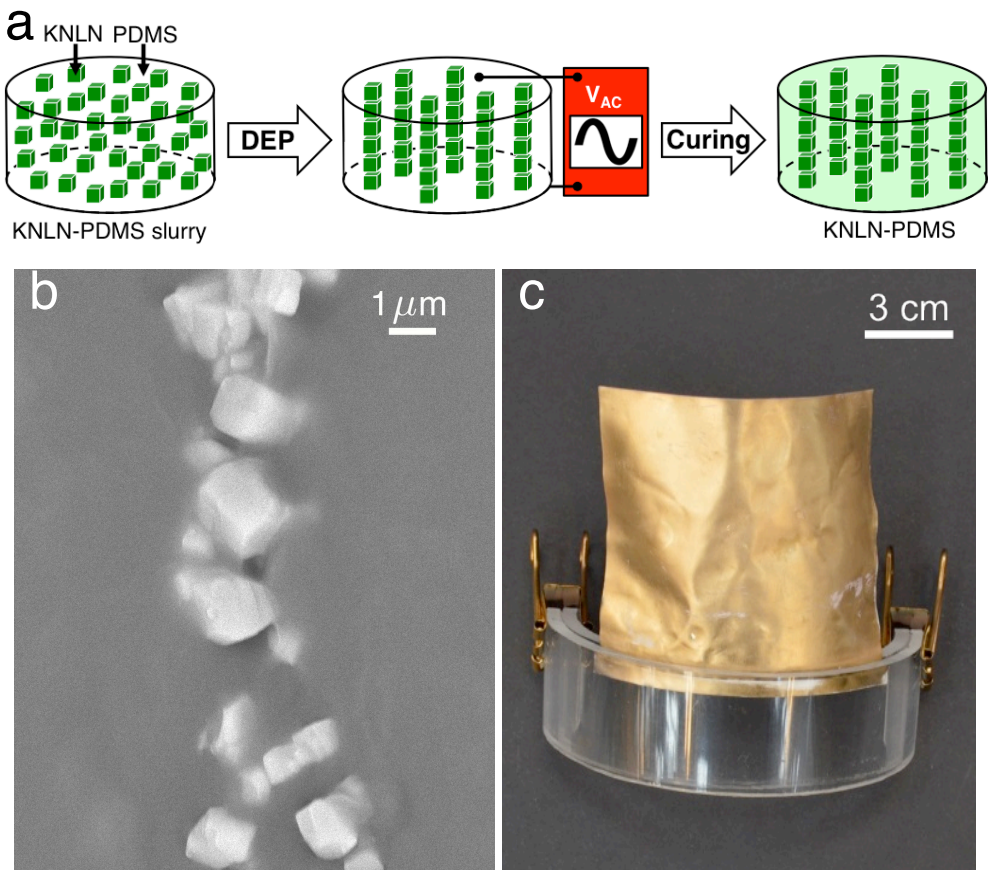

Figure 1. a) Schematic of the fabrication of aligned KNLN-PDMS composite films using dielectrophoresis. b) Scanning electron micrograph of a cross section of a cured and aligned KNLN-PDMS 5 vol.% composite, showing a single chain of aligned KNLN microcubes in the PDMS matrix. c) Large area 10 vol.% KNLN-PDMS composite film with Au electrodes sputtered on both sides, clamped between two sheets of curved plexiglass.

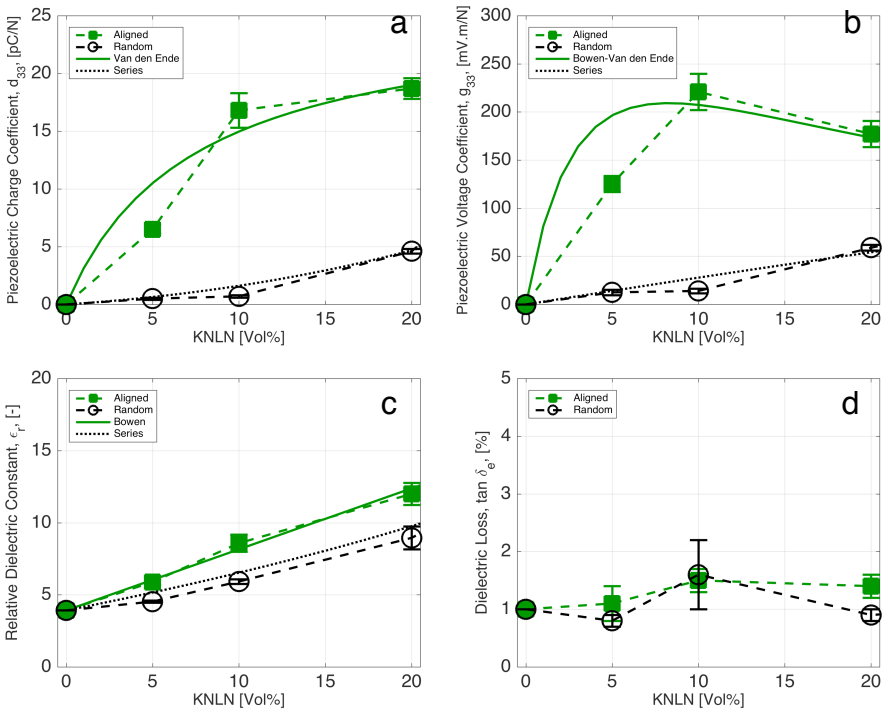

Figure 2. Piezoelectric constants of KNLN-PDMS composite films. a) Piezoelectric charge coefficient, d_{33}, as a function of KNLN content. b) Piezoelectric voltage coefficient, g_{33}, as a function of KNLN content. c) Relative dielectric constant, ε_r, as a function of KNLN content and d) Dielectric loss. Open circles represent randomly dispersed composite films, prepared without dielectrophoretic field. Solid squares represent dielectrophoretically aligned films. Dashed lines are a guide to the eye. Solid and dotted lines are quantitative fits to the data. The error bar at the optimal composition of 10 vol.% is extracted from averaging over more than 10 films.

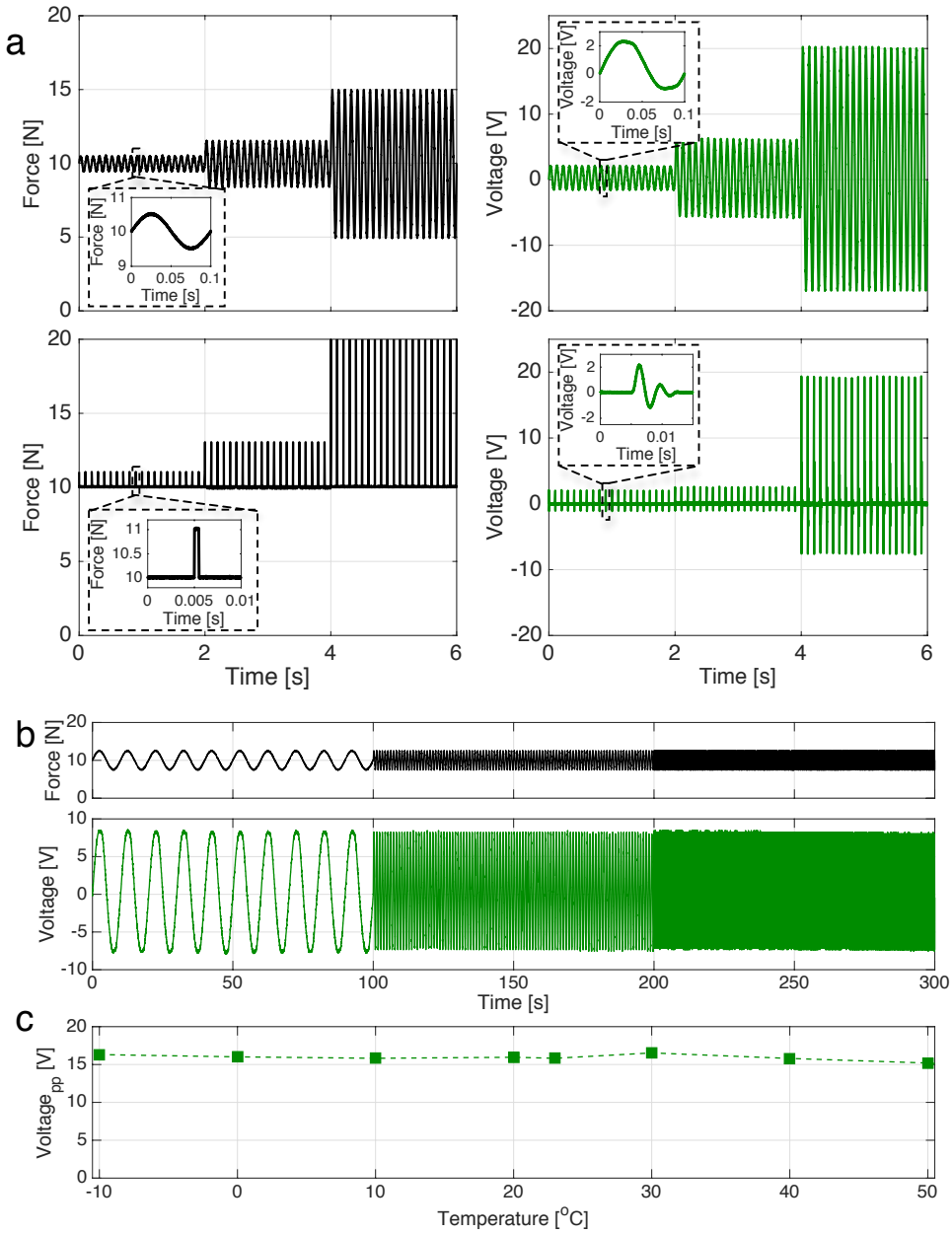

Figure 3. Voltage response of 1.1 mm thick, 8.7 mm diameter, composite disks of 10 vol.% dielectrophoretically aligned KNLN microcubes in a PDMS matrix, clamped with 10 N static force. a) Open circuit output voltage due to applied sinusoidal and pulse force of 1, 3 and 10 N. Inserts show the form of a single sinusoidal excitation and pulse excitation and the corresponding changes in open circuit voltage at 1 N peak to peak. b) Open circuit output voltage as a function of excitation frequency between 0.1 and 10 Hz. The applied force was 5 N. c) Open circuit output voltage as a function of temperature. The disk was excited with a sinusoidal force of 5 N. To exclude pyro-electric contributions, the disks were kept at each temperature for 30 minutes before measuring at 1 Hz in 100 s intervals.

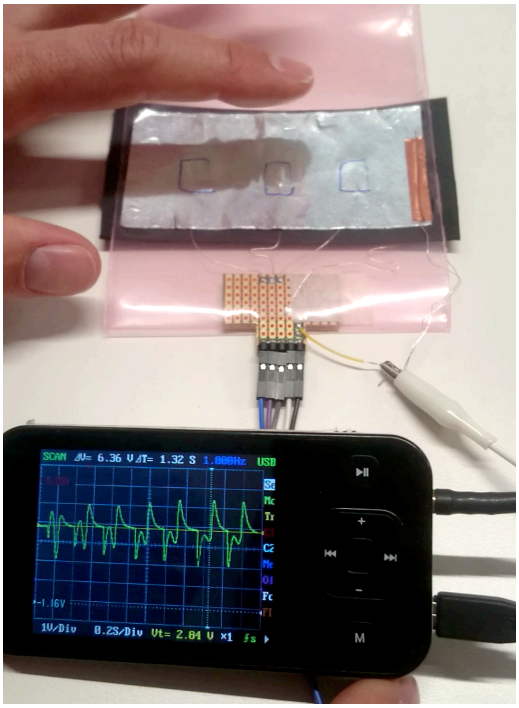

Figure 4. Flexible, state-of-the-art piezoelectric touch sensor based on a composite film of 10 vol.% dielectrophoretic aligned KNLN microcubes in a PDMS matrix. The handheld oscilloscope demonstrates the output voltage upon repeatedly touching the sensor. A video in the Supporting Information (Video S2) shows that even light tapping of the sensor generates enough voltage to accurately distinguish variations in touch intensity and speed.